



# Correction to: FoxD1-driven CCN2 deletion causes axial skeletal deformities, pulmonary hypoplasia, and neonatal asphyctic death

Lucas L. Falke<sup>1,2</sup> · Nannan He<sup>3</sup> · Susana M. Chuva de Sousa Lopes<sup>4</sup> · Roel Broekhuizen<sup>1</sup> · Karen Lyons<sup>5,6</sup> · Tri Q. Nguyen<sup>1</sup> · Roel Goldschmeding<sup>1</sup>

Published online: 14 April 2020  
© The International CCN Society 2020

Correction to: *Journal of Cell Communication and Signaling*  
<https://doi.org/10.1007/s12079-020-00549-4>

**Keywords** CCN2 · CTGF · FoxD1 · Lung · Hypoplasia · Skeletogenesis

## Introduction

Pulmonary fibrosis is a very severe and life-threatening disease characterized by interstitial fibrosis in the lung parenchyma leading to reduced lung and diffusion capacity, with consequent respiratory failure and often death. Fibrosis is the final common pathway of maladaptive tissue remodeling and loss of organ function.

Cellular Communication Network factor 2 (CCN2; also known as Connective Tissue Growth Factor, CTGF) is an important mediator of fibrosis in virtually all organs, including

the kidneys and the lungs (Pan et al. 2001; Wang et al. 2019). Myofibroblasts are the main effector cells during tissue fibrosis. Transformation of mesenchyme derived lung pericytes contributes importantly to the increase in myofibroblast numbers during pulmonary and kidney fibrosis, a process known to be CCN2 dependent (Shiwen et al. 2009; Hung et al. 2013).

The Fork head box D1 (FoxD1) transcription factor is transiently expressed in multiple mesenchymal cell types in several organs. FoxD1-derived mesenchymal cells, especially pericytes, contribute importantly to for example experimental kidney fibrosis and bleomycin induced pulmonary fibrosis

---

Publisher's note: Owing to a publisher error, the original version of this article, which can be found at [10.1007/s12079-020-00549-4](https://doi.org/10.1007/s12079-020-00549-4), was published with the incorrect version of the manuscript. To avoid any misinterpretation, the whole article is republished here in full. The publisher apologizes for any inconvenience caused.

---

**Electronic supplementary material** The online version of this article (<https://doi.org/10.1007/s12079-020-00559-2>) contains supplementary material, which is available to authorized users.

---

The online version of the original article can be found at <https://doi.org/10.1007/s12079-020-00549-4>

---

✉ Roel Goldschmeding  
R.Goldschmeding@umcutrecht.nl

<sup>1</sup> Department. Pathology, University Medical Centre Utrecht, Heidelberglaan, 100 3584 CX Utrecht, The Netherlands

<sup>2</sup> Department Internal medicine, Diaconessenhuis, Utrecht, the Netherlands

<sup>3</sup> Department Gynecology, the First Affiliated Hospital of Zhengzhou University, Zhengzhou, China

<sup>4</sup> Department Anatomy and Embryology, Leiden University Medical Center, Leiden, the Netherlands

<sup>5</sup> Department Orthopedic Surgery, University of California, Oakland, CA, USA

<sup>6</sup> Department Molecular Cell and Developmental Biology, University of California, Oakland, CA, USA

(Hung et al. 2013). In the lung CCN2 is also an important mediator of the pericyte-endothelial interface (Hall-Glenn et al. 2012).

In order to generate a tool for the study of CCN2 expression by FoxD1-lineage cells to fibrotic tissue remodeling, we set out to establish a colony of FoxD1cre-CCN2<sup>flox/flox</sup> mice. Surprisingly however, FoxD1cre-mediated homozygous CCN2 deletion induced an early postnatal fatal phenotype characterized by pulmonary hypoplasia and postnatal asphyxiation. Moreover, we observed subtle axial skeletal defects which might have led to reduced breathing movements in utero and subsequent lethal impairment of lung development.

## Materials and methods

### Animals

CCN2<sup>flox</sup> mice were a kind gift from dr. A. Leask. The generation processes of FoxD1Cre and CCN2<sup>flox</sup> mice has been described extensively elsewhere (Liu et al. 2011; Kobayashi et al. 2014). FoxD1Cre and homozygous CCN2<sup>flox</sup> mice were cross-bred at least 5 generations prior to conduction of experiments. FoxD1Cre - CCN2<sup>flox/flox</sup> pups were severely asphyctic and euthanized by decapitation. Heterozygous (FoxD1Cre-CCN2<sup>flox/+</sup>) littermates showed no abnormalities, consistent with lack of a spontaneous phenotype in heterozygous constitutive CCN2 knockouts (Ivkovic et al. 2003). In subsequent experiments, mothers were killed before delivery on embryonic day (E)18.5 to prevent confounding secondary postnatal pathology. All fetuses in these litters were killed by decapitation immediately after opening the womb.

### Immunohistochemistry

Whole embryos or selected tissues were embedded in paraffin blocks. Of these, 4  $\mu$ m sections were cut, mounted on object slides and deparaffinized/rehydrated using sequential rinsing in xylene and 100%, 90% and 70% EtOH. Hematoxylin and eosin (H&E) and periodic acid Schiff (PAS) staining were performed using standard protocols as used in diagnostics at the department of pathology.

CD31/PDGFR $\beta$  double staining was performed as followed: Citrate (pH 6) boiling antigen retrieval (20 min), PBS(T) rinsing, anti-CD31 primary antibody incubation (LS-B4737 (LS Bio, Seattle WA); 1:50, 1.5 h room temperature), PBS(T) rinsing, Brightvision-AP (Immunologic, Duiven, the Netherlands) secondary antibody incubation (1 h), PBS(T) rinsing, Liquid permanent red (ThermoFisher, Waltham, MA) substrate development, PBS rinsing, Citrate boiling antigen retrieval (10 min), PBS(T) rinsing, anti-PDGFR $\beta$  primary antibody incubation (NB100–57343 (Novus, Centennial, CO); 1:200, overnight 4 C), PBS(T) rinsing,

Brightvision-AP incubation (45 min), PBS(T) rinsing, Vector Blue (Vector, Burlingame, CA) substrate development, PBS rinsing, drying, xylene, coverslip.

### RT-qPCR

RNA was isolated from tissues using Trizol (ThermoFisher), and 3000 ng was reverse transcribed into cDNA. RT-qPCR was performed on a LightCycler480 (Roche, Basel, Switzerland), using commercially available TaqMan primer assays (Col1a2, Mm00483888\_m1; Ccn2, Mm01192933\_g1; Elastin, Mm00514692\_m1; Thermo Fisher). Using the delta-delta CT method, relative expression levels were calculated for each individual embryo, and the average expression levels of control embryos were set to 1.

### Genotyping PCR and gel electrophoresis

Samples were lysed using direct lyse buffer (Viagen, Los Angeles, CA) after which genotyping PCR was performed (Primers: CCN2 Flox: Forward: 5'- gAA ACA gCA ATT ACT ACA ACg ggA gTg g - 3', Reverse: 5'- gAA ACA gCA ATT ACT ACA ACg ggA gTg g - 3'. FoxD1 Cre: Forward Wild type: 5'- CTC CTC CGT GTC CTC GTC -3', Forward FoxD1 Cre: 5'- GGG AGG ATT GGG AAG ACA AT -3, Common reverse: 5'- TCT GGT CCA AGA ATC CGA AG -3'. After PCR, Midori green (Nippon Genetics, JPN) was added and samples were run on 1% agarose gel. For product size determination, a 1 kb PLUS DNA ladder (Invitrogen, cat no 10787–018) was used.

### Whole mount skeletal stain

Whole mount skeletal staining protocol of fetal carcasses is extensively described elsewhere (Rigueur and Lyons 2014). Briefly, wholemounts were rinsed, and fixed in ethanol (95%) and acetone respectively. Cartilage was stained by Alcian blue immersion, after which mounts were rinsed in 70% and 95% EtOH respectively. Using potassium hydroxide (KOH; 1% w/v), mounts were pre-cleared. Alizarin red was used to stain calcified bone. This was followed by immersion in KOH/glycerol (1:1) solution to remove excess red staining before storage in glycerol. Lordosis was measured as follows. Embryos were photographed after careful lateral positioning. Using the approximate same cervical vertebra in each mouse, straight lines were drawn fitting the axis of the upper cervical vertebrae and of the lower vertebrae/ upper thoracic vertebrae. Using ImageJ, the angle between x and y was determined.

### Statistics

Statistical significance between groups was tested using the Student-T test using GraphPad Prism Version 8.0.1

(GraphPad, San Diego, CA). A *P* value below 0.05 was considered statistically significant. Error bars represented SEM.

**Ethics** All experiments were conducted with permission of the animal ethics committee of the University of Utrecht.

## Results

### FoxD1Cre driven CCN2 deletion leads to impaired lung development and postnatal asphyxia but unaltered expression of structural proteins

Upon birth, FoxD1Cre/CCN2<sup>flox/flox</sup> pups showed a slight thoracic kyphosis and made gasping movements, became cyanotic and severely asphyctic (Supplemental Video 1). They were euthanized by decapitation. Body weight after birth was similar in both FoxD1Cre/CCN2<sup>flox/flox</sup> and WT/CCN2<sup>flox/flox</sup> groups (average 1.4-g, SEM ± 0.3). However, the lung to body weight ratio was reduced in FoxD1Cre/CCN2<sup>flox/flox</sup> mice (WT/CCN2<sup>flox/flox</sup>: 41.58 mg/g SEM ± 1.28 and FoxD1Cre/CCN2<sup>flox/flox</sup>: 36.23 mg/g SEM ± 1.49 respectively; *P* < 0.05).

Analysis of PAS stained lung sections showed reduced potential airspace compared to WT/CCN2<sup>flox/flox</sup> mice (*P* < 0.05; Fig. 1A and B). CD31 (endothelium) and PDGFRβ (pericytes) revealed no aberrancies in the endothelial/pericyte interface in FoxD1Cre/CCN2<sup>flox/flox</sup> mice (Fig. 1C).

Type I pneumocytes are the most abundant cell type in the lungs. *Podoplanin* mRNA expression level as a surrogate marker for type I pneumocyte numbers, showed no difference between WT/CCN2<sup>flox/flox</sup> and FoxD1Cre/CCN2<sup>flox/flox</sup> mice (Fig. 1D).

The expression of *Collα2* mRNA was not significantly different (Fig. 1E), and also hydroxyproline/proline content was similar in both groups (Fig. 1F). The expression level of *Elastin* mRNA was significantly reduced in FoxD1Cre/CCN2<sup>flox/flox</sup> mice (*P* < 0.05; Fig. 1G), but mass spectrometry analysis of isodesmin as a marker for elastin fibrils showed no significant difference (Fig. 1H).

### CCN2 deletion in FoxD1-lineage derived cells in the lung does not affect pulmonary CCN2 mRNA expression level at late gestation

CCN2<sup>flox</sup> genotyping PCR of lung parenchyma at E18.5 shows a profound knock-out (KO) DNA band in FoxD1Cre positive CCN2<sup>flox/flox</sup> mice (Fig. 2A), indicating FoxD1Cre driven CCN2 recombination has occurred before E18.5. However, at E18.5 total pulmonary *Ccn2* mRNA expression was not significantly lower compared to WT/CCN2<sup>flox</sup> mice (*P* = 0.07; Fig. 2B). This suggests that the contribution

pulmonary FoxD1 lineage cells make to CCN2 production in the lung at this late developmental stage is limited.

### Disturbance of axial skeleton development in FoxD1Cre/CCN2<sup>flox</sup> mice

In whole mount Alcian blue/Alizarin red stained skeletons, cervical lordosis was increased in FoxD1Cre/CCN2<sup>flox/flox</sup> compared to WT/CCN2<sup>flox/flox</sup> pups (Fig. 3A&B; *P* < 0.01). Additionally, the sternal length of FoxD1Cre/CCN2<sup>flox/flox</sup> mice was significantly shorter when compared to WT/CCN2<sup>flox</sup> mice (Fig. 3C&D; *P* < 0.05).

Global microscopic assessment of Alcian blue, Collagen type 2 and Ki67 (immuno)histochemistry however showed no apparent differences in FoxD1Cre/CCN2<sup>flox/flox</sup> compared to the WT/CCN2<sup>flox/flox</sup> littermates (data not shown).

CCN2<sup>flox</sup> PCR showed a much more pronounced KO band in fetal tail-, than liver DNA, suggesting that FoxD1-lineage cells contribute significantly to CCN2-expression during axial skeletal development (Fig. 3E).

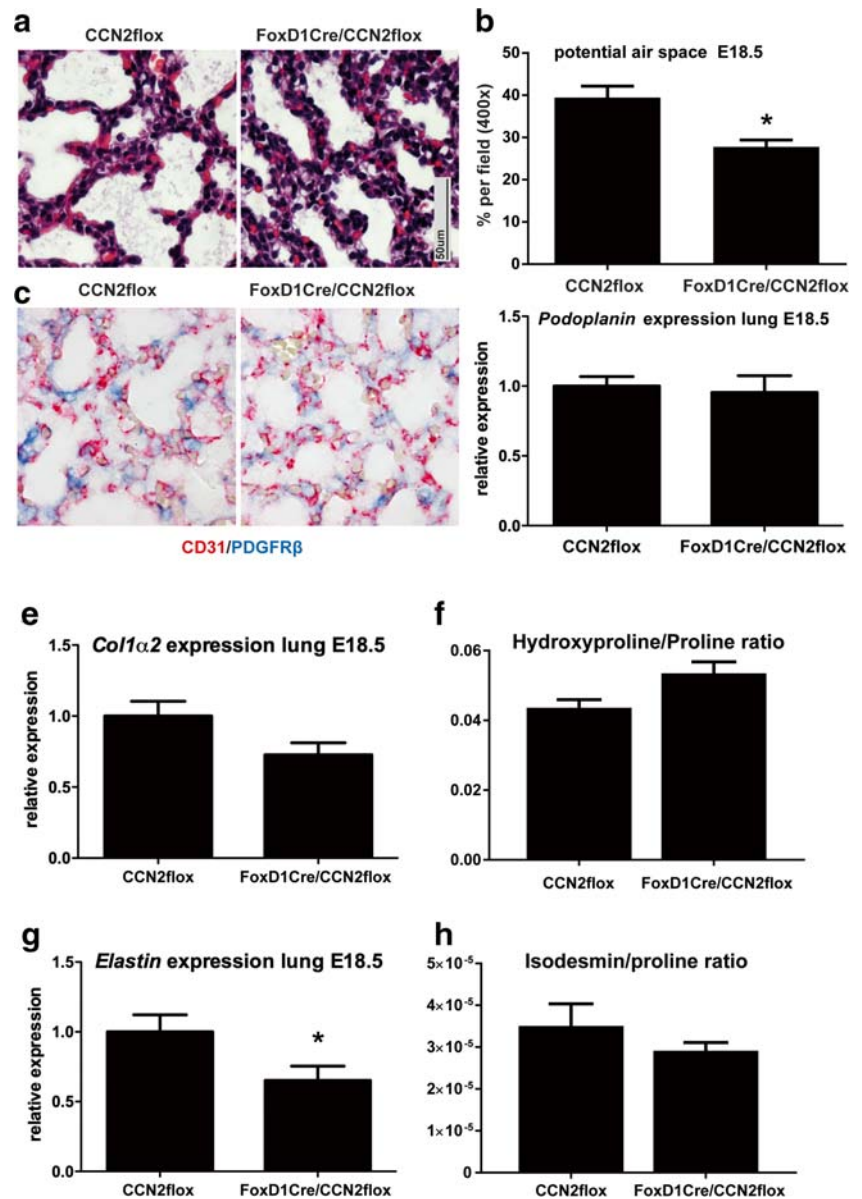
## Discussion

Here we show that loss of CCN2 from FoxD1-lineage cells leads to aberrant lung morphology with post-natal asphyxiation, and axial skeletal deformities.

In postnatal lungs, CCN2 is mainly expressed in terminal bronchiolar epithelium (Burgos et al. 2010), which does not derive from FoxD1 expressing progenitor cells (Hung et al. 2013). This explains why *Ccn2* expression levels are not altered significantly in E18.5 FoxD1Cre/CCN2<sup>flox/flox</sup> lungs (Fig. 2). The lung hypoplasia in our FoxD1Cre/CCN2<sup>flox/flox</sup> mice is very similar to that in constitutive CCN2-knock out mice. CCN2 is expressed in the developing lung (Burgos et al. 2010), and it has been proposed that in constitutive CCN2 – KO mice the absence of pulmonary CCN2 expression in the developing lung itself contributes importantly to pulmonary hypoplasia (Baguma-Nibasheka and Kablar 2008), but the lung hypoplasia in constitutive CCN2-knock out mice has also been interpreted as being secondary to their profound skeletal deformities (Ivkovic et al. 2003; Baguma-Nibasheka and Kablar 2008).

Normal lung development requires a structurally well-developed thorax (Inanlou et al. 2005) (Cameron et al. 2009). As an important regulator of enchondral ossification, CCN2 is critically involved in normal skeletal development as evidenced by severe malformations in constitutive CCN2-knockout mice (Kubota and Takigawa 2007) (Ivkovic et al. 2003; Baguma-Nibasheka and Kablar 2008). Similarly, the axial skeletal deformities in our FoxD1Cre/CCN2<sup>flox/flox</sup> mice are most likely the direct effect of CCN2 silencing in FoxD1-lineage cells in the

**Fig. 1** – Impaired lung development without structural protein alterations in FoxD1/CCN2floxed embryos: **A**) H&E staining of CCN2floxed (WT) and FoxD1Cre/CCN2floxed (KO) pulmonary parenchyma at embryonic day 18.5. **B**) Quantification of potential airspace (%), **C**) CD31 (red) and PDGFR $\beta$  (blue) immunohistochemistry, **D**) *Podoplanin* mRNA expression, **E**) *Col1 $\alpha$ 2* mRNA expression, **F**) Hydroxyproline/proline ratio, **G**) *Elastin* mRNA expression and **H**) Isodesmin/proline ratio of WT and KO lungs. SEM shown. \* represents a *P* value <0.05 (Student T-test). *N* = 4 per group



developing axial skeleton. This would also be consistent with the reported co-segregation of a human chromosome region spanning 5q13.2 to 13.4 including the FOXD1

gene, as a locus co-segregating with disease in multiple generations of a family with idiopathic scoliosis (Edery et al. 2011).

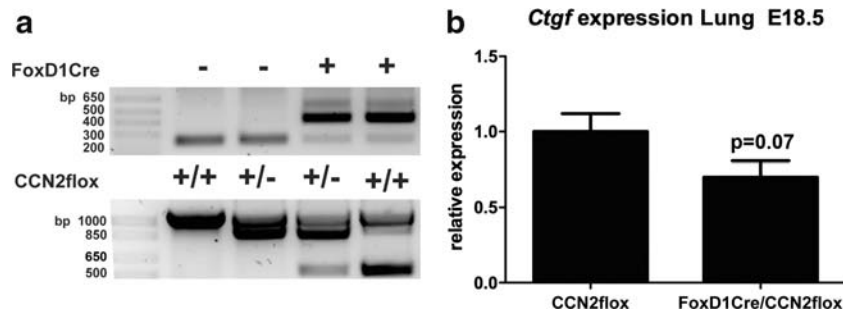
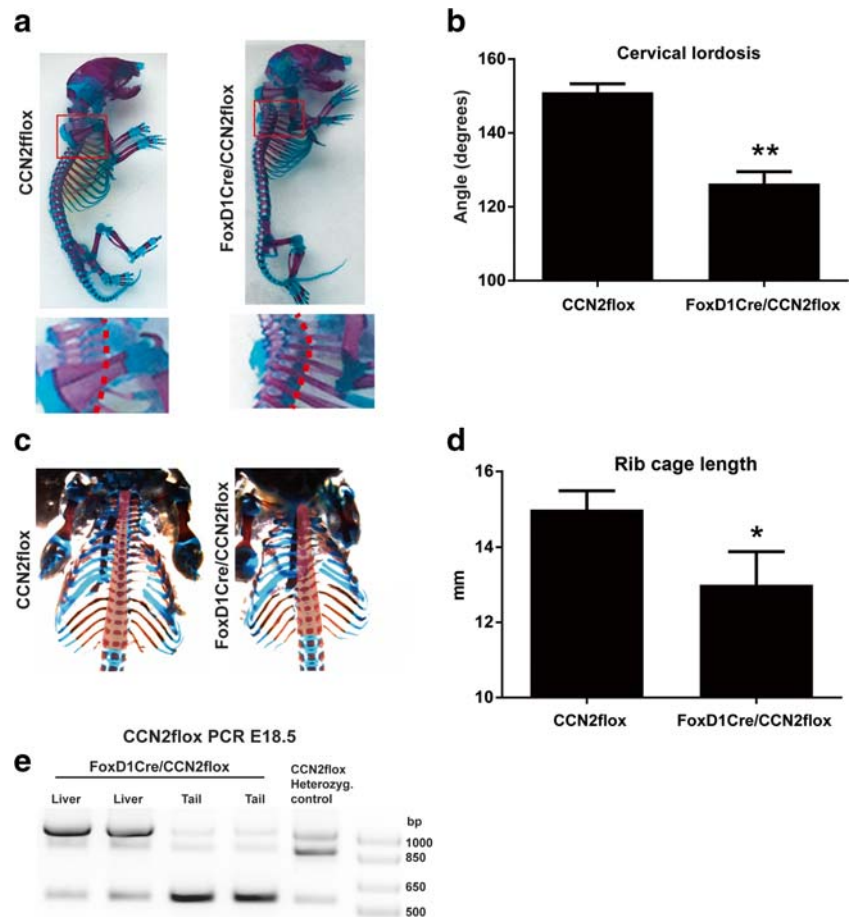


**Fig. 2** – FoxD1Cre driven CCN2 DNA deletion slightly and non-significantly reduces pulmonary *Ccn2* expression: **A**) FoxD1Cre and CCN2floxed genotypes in homo- and heterozygous CCN2floxed mice with

or without FoxD1 (CCN2 lower band represents KO product). **B**) *Ccn2* mRNA expression level of WT and KO lungs. SEM shown. *N* = 4 per group

**Fig. 3** – FoxD1/CCN2<sup>flx</sup> embryos show subtle skeletal deformities: **A)** Whole mount Alcian blue (cartilage)/Alizarin red (bone) skeletal stain of CCN2<sup>flx</sup> (WT) and FoxD1Cre/CCN2<sup>flx</sup> (KO) embryos. Lower micrographs showing cervicothoracic lordosis; dotted line represents measured angle. **B)** Quantification of cervicothoracic lordosis. **C)** Representative images and **D)** Quantification of WT and KO rib cage lengths in mm. **E)** Gel electrophoresis of CCN2<sup>flx</sup> in cartilaginous tail tissue of KO embryos showing near total genomic KO recombination of CCN2 compared to liver. SEM shown. \* represents  $P < 0.05$ , \*\* represents  $P < 0.01$  (Student T-test).  $N = 3$  per group



The similarity of the pulmonary phenotype of constitutive CCN2-knock out mice with the impaired development of fetal lungs of FoxD1Cre/CCN2<sup>flx/flx</sup> embryos in the current study suggests that also in the latter lung hypoplasia might have developed secondary to the skeletal deformities.

In summary, we report that targeted CCN2 deletion in cells expressing FoxD1 during embryonic development leads to a lethal phenotype associated with axial skeletal deformities and postnatal asphyxiation due to (possibly secondary) pulmonary hypoplasia.

**Acknowledgements** We thank dr. A. Leask for the kind donation of CCN2<sup>flx/flx</sup> mice.

## References

- Baguma-Nibasheka M, Kablar B (2008) Pulmonary hypoplasia in the connective tissue growth factor (Ctgf) null mouse. *Dev Dyn* 237: 485–493. <https://doi.org/10.1002/dvdy.21433>
- Burgos CM, Nord M, Roos A, Didon L, Eklöf AC, Frenckner B (2010) Connective tissue growth factor expression pattern in lung development. *Exp Lung Res* 36:441–450. <https://doi.org/10.3109/01902141003714056>
- Cameron TL, Belluocchio D, Farlie PG et al (2009) Global comparative transcriptome analysis of cartilage formation in vivo. *BMC Dev Biol* 9:20–17. <https://doi.org/10.1186/1471-213X-9-20>
- Ederly P, Margaritte-Jeannin P, Biot B, Labalme A, Bernard JC, Chastang J, Kassai B, Plais MH, Moldovan F, Clerget-Darpoux F (2011) New disease gene location and high genetic heterogeneity in idiopathic scoliosis. *Eur J Hum Genet* 19:865–869. <https://doi.org/10.1038/ejhg.2011.31>
- Hall-Glenn F, De Young RA, Huang B-L et al (2012) CCN2/connective tissue growth factor is essential for pericyte adhesion and endothelial basement membrane formation during angiogenesis. *PLoS One* 7: e30562. <https://doi.org/10.1371/journal.pone.0030562>
- Hung C, Linn G, Chow Y-H, Kobayashi A, Mittelsteadt K, Altemeier WA, Gharib SA, Schnapp LM, Duffield JS (2013) Role of lung pericytes and resident fibroblasts in the pathogenesis of pulmonary fibrosis. *Am J Respir Crit Care Med* 188:820–830. <https://doi.org/10.1164/rccm.201212-2297OC>
- Inanlou MR, Baguma-Nibasheka M, Kablar B (2005) The role of fetal breathing-like movements in lung organogenesis. *Histology and Histopathology* 20(4):1261–1266. <https://doi.org/10.14670/HH-20.1261>
- Ivkovic S, Yoon BS, Popoff SN, Safadi FF, Libuda DE, Stephenson RC et al. (2003) Connective tissue growth factor coordinates chondrogenesis and angiogenesis during skeletal development. *Development (Cambridge, England)* 130(12):2779–2791
- Kobayashi A, Mugford JW, Krautzberger AM, Naiman N, Liao J, McMahon A (2014) Identification of a multipotent self-renewing stromal progenitor population during mammalian kidney

- organogenesis. *Stem Cell Reports* 3:650–662. <https://doi.org/10.1016/j.stemcr.2014.08.008>
- Kubota S, Takigawa M (2007) Role of CCN2/CTGF/Hcs24 in bone growth. *Int Rev Cytol* 257:1–41. [https://doi.org/10.1016/S0074-7696\(07\)57001-4](https://doi.org/10.1016/S0074-7696(07)57001-4)
- Liu S, Shi-wen X, Abraham DJ, Leask A (2011) CCN2 is required for bleomycin-induced skin fibrosis in mice. *Arthritis Rheum* 63:239–246. <https://doi.org/10.1002/art.30074>
- Pan LH, Yamauchi K, Uzuki M, Nakanishi T, Takigawa M, Inoue H, Sawai T (2001) Type II alveolar epithelial cells and interstitial fibroblasts express connective tissue growth factor in IPF. *Eur Respir J* 17:1220–1227. <https://doi.org/10.1183/09031936.01.00074101>
- Rigueur D, Lyons KM (2014) Whole-mount skeletal staining. *Methods Mol Biol* 1130:113–121. [https://doi.org/10.1007/978-1-62703-989-5\\_9](https://doi.org/10.1007/978-1-62703-989-5_9)
- Shiwen X, Rajkumar V, Denton CP, Leask A, Abraham DJ (2009) Pericytes display increased CCN2 expression upon culturing. *J Cell Commun Signal* 3:61–64. <https://doi.org/10.1007/s12079-009-0053-7>
- Wang X, Cui H, Wu S (2019) CTGF: a potential therapeutic target for Bronchopulmonary dysplasia. *Eur J Pharmacol* 860:172588. <https://doi.org/10.1016/j.ejphar.2019.172588>

**Publisher's note** Springer Nature remains neutral with regard to jurisdictional claims in published maps and institutional affiliations.